

# The cytochrome $c_3$ –[Fe]-hydrogenase electron-transfer complex: structural model by NMR restrained docking

Latifa ElAntak<sup>a</sup>, Xavier Morelli<sup>a</sup>, Olivier Bornet<sup>a</sup>, Claude Hatchikian<sup>a</sup>, Mirjam Czjzek<sup>b</sup>,  
Alain Dolla<sup>a</sup>, Françoise Guerlesquin<sup>a,\*</sup>

<sup>a</sup>Unité de Bioénergétique et Ingénierie des Protéines, IBSM-CNRS, 31 chemin Joseph Aiguier, 13402 Marseille Cedex 20, France

<sup>b</sup>Unité de Architecture et Fonction des Macromolécules Biologiques, IBSM-CNRS, 31 chemin Joseph Aiguier, 13402 Marseille Cedex 20, France

Received 15 April 2003; accepted 16 May 2003

First published online 4 July 2003

Edited by Thomas L. James

**Abstract** Cytochrome  $c_3$  ( $M_r$  13 000) is a low redox potential cytochrome specific of the anaerobic metabolism in sulfate-reducing bacteria. This tetrahemic cytochrome is an intermediate between the [Fe]-hydrogenase and the cytochrome Hmc in *Desulfovibrio vulgaris* Hildenborough strain. The present work describes the structural model of the cytochrome  $c_3$ –[Fe]-hydrogenase complex obtained by nuclear magnetic resonance restrained docking. This model connects the distal cluster of the [Fe]-hydrogenase to heme 4 of the cytochrome, the same heme found in the interaction with cytochrome Hmc. This result gives evidence that cytochrome  $c_3$  is an electron shuttle between the periplasmic hydrogenase and the Hmc membrane-bound complex.

© 2003 Published by Elsevier Science B.V. on behalf of the Federation of European Biochemical Societies.

**Key words:** Electron transfer; Cytochrome; [Fe]-hydrogenase; NMR; Docking

## 1. Introduction

Molecular hydrogen plays a central role in the metabolic activity of many *Desulfovibrio* species, used as the sole source of electron and energy [1] or produced in the absence of terminal electron acceptors [2]. The couple hydrogenase/cytochrome  $c$  is the key system for hydrogen metabolism in *Desulfovibrio*. The two components work in tandem, hydrogenase being the enzyme catalyzing the splitting or the synthesis of molecular hydrogen and cytochrome  $c$  acting as the electron and proton transport protein [3].

The three-dimensional structure of *Desulfovibrio desulfuricans* ATCC 7757 [Fe]-hydrogenase [4], identical to *Desulfovibrio vulgaris* Hildenborough enzyme [5], has been determined by X-ray crystallography. [Fe]-hydrogenase is composed of two subunits of 42 and 10 kDa, respectively. The large subunit contains a ferredoxin-like domain with two [4Fe–4S] clusters and a so-called H cluster constituted of a regular [4Fe–4S] cluster bridged to an active site Fe binuclear center.

Cytochrome  $c_3$  ( $M_r$  13 000) is a periplasmic low redox potential cytochrome uniformly present in *Desulfovibrio* species and characterized by the presence of four *bis*-histidinyl axial-

coordinated heme groups covalently bound to the polypeptide chain by two thioether bridges. Cytochrome  $c_3$  works as a coupling protein to periplasmic hydrogenase and has been involved in a concerted proton-assisted two-electron step [3]. Cytochromes  $c_3$  from several *Desulfovibrio* species have been extensively studied both biochemically and structurally. Despite a low sequence identity, their three-dimensional structures are very well conserved, designing thus a typical arrangement of the heme core for this class of molecule ([6] and references therein). *Desulfovibrio* cells may contain other soluble multiheme cytochromes, among which the high molecular weight cytochrome (Hmc) [7]. In *D. vulgaris* Hildenborough, biochemical and kinetics studies have shown that the tetraheme cytochrome  $c_3$  ( $M_r$  13 000) mediates the reduction of Hmc by the [Fe]-hydrogenase [8,9]. We have recently solved by X-ray diffraction the structure of the 16 hemes containing cytochrome (Hmc) from *D. vulgaris* Hildenborough and obtained a structural model of the Hmc–cytochrome  $c_3$  complex by nuclear magnetic resonance (NMR) restrained docking [10].

In the present work, we present the structural model of the [Fe]-hydrogenase–cytochrome  $c_3$  complex, obtained by the same approach, combining heteronuclear NMR titration of the complex formation, and ab initio calculation of the docking of the two molecules by the software BiGGER [11].

## 2. Materials and methods

### 2.1. NMR samples

<sup>15</sup>N-labeled cytochrome  $c_3$  ( $M_r$  13 000) (further referred to as cytochrome  $c_3$ ) from *D. vulgaris* Hildenborough and *D. desulfuricans* ATCC 7757 [Fe]-hydrogenase were obtained as previously reported [12] and [13], respectively). NMR experiments were carried out at 296 K, with a cytochrome  $c_3$  concentration of 37  $\mu$ M, in the presence of zero, one and two equivalents of [Fe]-hydrogenase.

### 2.2. NMR experiments

<sup>15</sup>N–<sup>1</sup>H HSQC experiments were recorded on a Bruker Avance DRX500 spectrometer, equipped with a HCN probe and self-shielded triple-axis gradients. Spectra were acquired accumulating 224 scans per free induction decay, with 256 complex points in F1 and 2K complex points in F2. The spectral widths were 6 kHz in F2 and 2 kHz in F1. <sup>1</sup>H chemical shifts were referenced with H<sub>2</sub>O resonance calibrated at 4.792 ppm and <sup>15</sup>N chemical shifts were referenced indirectly using the <sup>1</sup>H/<sup>15</sup>N frequency ratio 0.1013291118 [14]. Spectrum processing was done with XwinNMR from Bruker and they were analyzed using Felix from Accelrys ([www.accelrys.com](http://www.accelrys.com)). <sup>15</sup>N and <sup>1</sup>H chemical shift assignments of cytochrome  $c_3$  have been previously reported (accession number BMRB-5239).

\*Corresponding author. Fax: (33)-4-91 16 45 78.

E-mail address: [guerlesq@ibsm.cnrs-mrs.fr](mailto:guerlesq@ibsm.cnrs-mrs.fr) (F. Guerlesquin).

### 2.3. Protein docking and NMR filtering

Molecular interaction simulations were obtained using the docking program BiGGER [11]. This algorithm performs a complete and systematic search in the binding space of both molecules. The solutions were then clustered and ranked according to the scoring function developed in BiGGER. The 1000 solutions obtained from BiGGER were analyzed using the NMR constraints.

### 2.4. Molecular dynamics and minimization of the structures of the complex

The best structures were minimized using the X-PLOR 3.851 program. Then, a molecular dynamics calculation (AMBER force field) was performed on the selected complex structures. All the metal centers and [4Fe–4S] clusters were tightly constrained with the SHAKE algorithm [15] allowing a tolerance of 0.0004. The coordinates of the best structure have been deposited at the Protein Data Bank (pdb ID: 1gx7).

## 3. Results

### 3.1. NMR mapping of the interacting site

Chemical shift perturbation is the most widely used NMR method to map protein interfaces [16]. The interaction causes environmental changes on the protein interfaces and, hence, affects the chemical shifts of the nuclei in this area.  $^1\text{H}$ – $^{15}\text{N}$  HSQC experiments have been recorded (Fig. 1A), in the absence and in the presence of stoichiometric amounts of unlabeled [Fe]–hydrogenase. Only few residues were affected by the complex formation, indicating that the entire protein did not undergo conformational change. These residues correspond to the protein–protein interface. The mapping of the interacting site has been obtained from the induced  $^1\text{H}$  and  $^{15}\text{N}$  chemical shifts observed on the cytochrome  $c_3$  NH resonances. The behavior of the NMR resonances (averaged value between the resonances of the free and bound cytochrome  $c_3$ ) are in agreement with a fast exchange process on the NMR time scale, generally observed for transient electron-transfer complexes. The proton and nitrogen chemical shift changes are equivalent to those observed in other complexes [17,18], ranging up to 0.036 ppm for  $^1\text{H}$  and up to 0.175 ppm for  $^{15}\text{N}$ . The  $^{15}\text{N}$  and  $^1\text{H}$  chemical shift variations were balanced as previously described [19]. 11 residues presenting a significant variation, higher than the relative value of 0.6 (Fig. 1B), were retained for the NMR filtering (residues 38, 46, 53, 59, 70, 72, 78, 81, 96, 98 and 99).

### 3.2. Docking of the complex

An ab initio docking of the cytochrome  $c_3$ –[Fe]–hydrogenase complex was calculated using the BiGGER software, on the basis of the Protein Data Bank coordinates from *D. vulgaris* Hildenborough cytochrome  $c_3$  (2cth) and *D. desulfuricans* [Fe]–hydrogenase (1hfe). 1000 putative structures

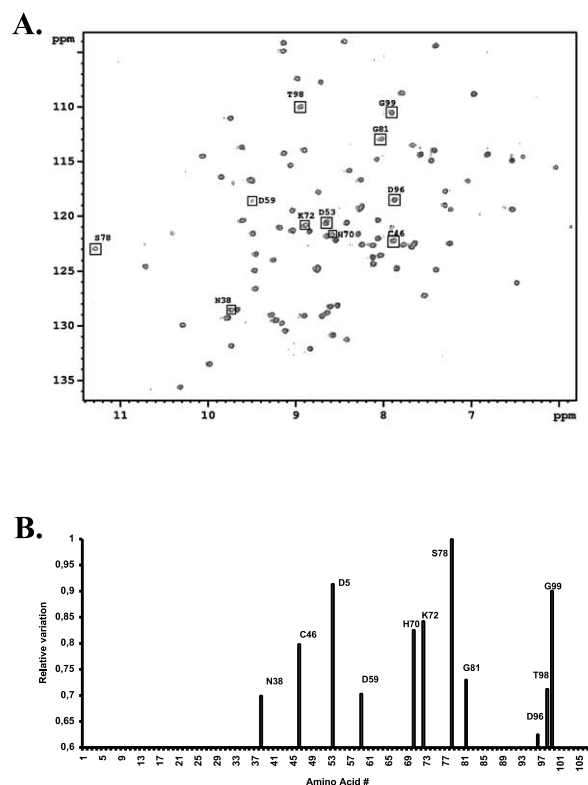


Fig. 1. A: Superposition of the  $^1\text{H}$ – $^{15}\text{N}$  HSQC spectra of the cytochrome  $c_3$  in the absence and in the presence of [Fe]–hydrogenase at a ratio of 1:1. The NH groups affected by the complex formation are in boxes and labeled according to the cytochrome  $c_3$  sequence numbering. B: Chemical shift variations observed from panel A. The relative variations of  $^1\text{H}$  and  $^{15}\text{N}$  were calculated according to [19].

were generated and selected, based on the geometric complementarity and amino acid pairwise affinities between the two molecular surfaces. In a subsequent step, the putative docked structures are ranked using an interaction scoring function (Fig. 2A), which combines several interaction terms that are thought to be relevant for the stabilization of protein complexes: geometric packing of surfaces, explicit electrostatic interactions, desolvation energy and pairwise propensities of amino acid side chains to interact across the molecular interface. These structures were then selected using the data of the NMR mapping, considering that an NH group is affected if it is at least at a distance of 5 Å of any atom belonging to the other protein. The solutions were ranked according to the level of agreement with the NMR data. The top 30 retained solutions were analyzed according to the heme/iron distances

Table 1

Comparison of structural characteristics of the five final models of the cytochrome  $c_3$ –hydrogenase complex

No.	Bigger score without NMR filter	NMR restraints	Fe–Fe distance heme/cluster (Å)	Global interacting surface/ (cytochrome surface only) (Å) <sup>2</sup>	Percentage of polar/apolar contacts on the interface <sup>a</sup> (%)	Energy (kcal mol <sup>−1</sup> )
1	85.30	8	8.8	2236.9/1088.9	35/65	−23 918
2	71.89	7	13.2	2076.1/1035.1	28/72	−23 934
3	70.45	7	8.8	2397.8/1183.6	32/68	−24 001
4	78.56	7	12.1	2352.8/1150.8	41/59	−23 984
5	69.45	7	10.9	2559.8/1236.3	40/60	−23 952

The values listed here were obtained after energy minimization.

<sup>a</sup>The ratio of polar to apolar interactions at the interface was calculated at the website <http://www.biochem.ucl.ac.uk/bsm/PP/server/>.

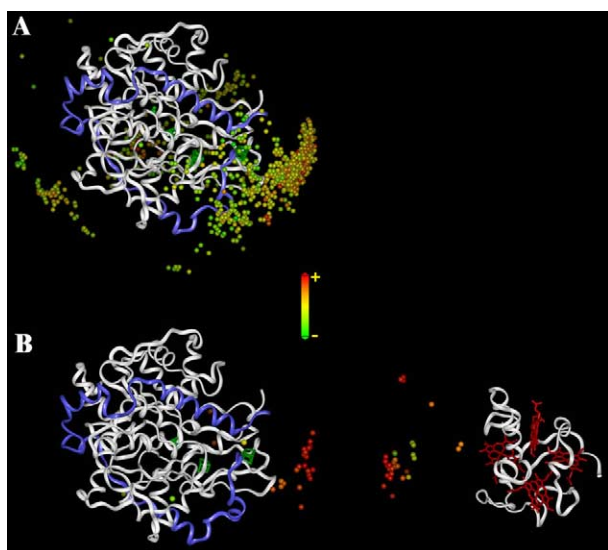


Fig. 2. Docking of cytochrome  $c_3$ -[Fe] hydrogenase complex. A: Ab initio docking. The structure of [Fe]-hydrogenase is shown as a ribbon trace (the large subunit is in white and the small one in blue). The center of mass of the cytochrome, in each of the 1000 putative docking solutions, is represented by a small sphere. The spheres are colored according to the relative ab initio interaction score of the corresponding solution. B: Top 30 solutions of the ab initio docking filtered by NMR mapping restraints. At the left, the [Fe]-hydrogenase structure is represented as a ribbon trace and the center of mass of the cytochrome as a small sphere. The solutions are color-coded according to the distance between one of the hemes of cytochrome  $c_3$  and one of the clusters of [Fe]-hydrogenase. At the right, the 30 docking solutions, with cytochrome  $c_3$  structure shown as a ribbon trace, and the center of mass of the [Fe]-hydrogenase is represented by small spheres.

(Fig. 2B). The top 10 solutions involve heme 4 of cytochrome  $c_3$  and the distal cluster of the [Fe]-hydrogenase. These solutions were clustered in five families with respect to their geometries (Table 1).

Solution 1 has the best score from the BiGGER scoring function, the highest NMR score, the shortest heme-FeS distance, and the most favorable polar/apolar contacts at the interface. Solution 1 has, thus, been selected as the best representative structure of the cytochrome  $c_3$ -[Fe]-hydrogenase complex and the model is presented in Fig. 3A.

#### 4. Discussion

The structural model of the [Fe]-hydrogenase and cytochrome  $c_3$  complex (Fig. 3A) presents a contact surface of  $2236 \text{ \AA}^2$ , which is similar to the value found for the cytochrome  $c_{553}$ -[Fe]-hydrogenase complex [20]. The interacting surfaces between cytochrome  $c_3$  and [Fe]-hydrogenase are highly complementary, as is exemplified by the side chain of I36 from hydrogenase, which fills up a cavity close to heme 4 of the cytochrome on its surface-exposed side. The side chain atoms of I36, highly conserved among ferredoxins and ferredoxin-like domains of hydrogenases, are within van der Waals distances to atoms of ring B of heme 4 (Fig. 3B). Besides the above mentioned I36 of hydrogenase, a tyrosine residue (Y66) of the cytochrome  $c_3$ , parallel to the sixth axial ligand histidine of heme 4, is at the center of the interface, pointing toward residues of the hydrogenase surrounding the distal [4Fe-4S] cluster; moreover, Y66 is in close contact with

C38, ligand of the distal [4Fe-4S] cluster. In the [Fe]-hydrogenase and cytochrome  $c_3$  complex a rather short distance is observed between the sulfur atoms of cysteines, namely C100 covalently linked to the heme group of the cytochrome  $c_3$  with respect to C76 (4.52  $\text{\AA}$ ) and C38 (5.5  $\text{\AA}$ ), two ligands of the distal [4Fe-4S] cluster of the hydrogenase (Fig. 3C). Apparently, this interaction leads to a favorable electron-transfer pathway across the intermolecular surfaces and thus, the relative orientation of the heme/FeS interface seems to be a common feature of numerous electron-transfer complexes [17,20]. In the cytochrome  $c_3$ -hydrogenase complex, the distance between heme 4 and the distal cluster is very short (8.8  $\text{\AA}$ ) compared to the distance found in other complexes like cytochrome  $c_{553}$ -hydrogenase (12.3  $\text{\AA}$ ). The large difference is obviously due to the high exposure of heme 4 to the solvent ( $150 \text{ \AA}^2$ ) as compared to the exposure of the heme of cytochrome  $c_{553}$  ( $50 \text{ \AA}^2$ ), making a direct involvement of the exposed heme edge (porphyrin rings A and B) in intermolecular contacts possible (the distance I36 CB to heme 4 CMB is 4.1  $\text{\AA}$ ). Since it is not the heme edge carrying the propionate groups of heme 4 which is involved in the interface, the propionates come to lie near the interacting surface but are not involved in electrostatic interactions in the model.

In the present work, we give evidence that [Fe]-hydrogenase transfers electrons to cytochrome  $c_3$  through heme 4, which plays the role of the electron entrance gate of the cytochrome.

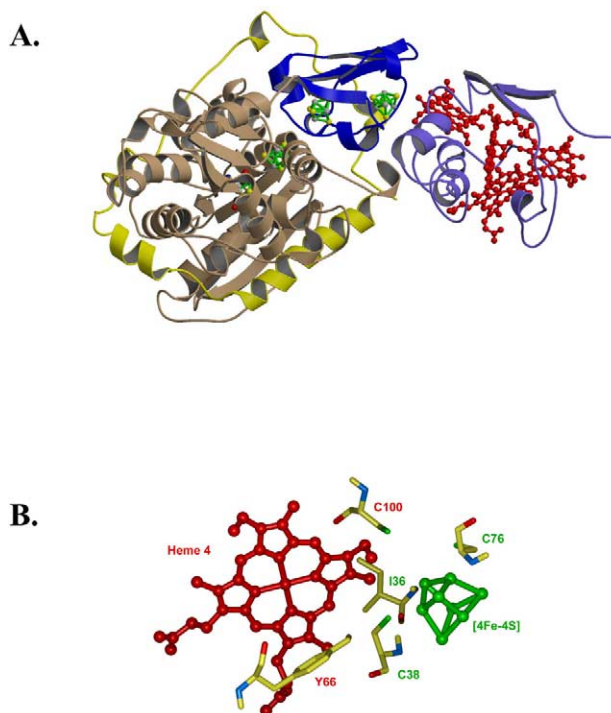


Fig. 3. A: Ribbon representation of the best representative structure of the [Fe]-hydrogenase-cytochrome  $c_3$  complex. The [Fe]-hydrogenase is the left polypeptide chain, the large subunit is colored in beige; the small subunit is colored in yellow and the ferredoxin-like domain in blue, the iron clusters are in green. Cytochrome  $c_3$  is the right polypeptide chain colored in blue, the heme groups are in red. B: Zoom-in view of the interface region, highlighting the residues involved in interatomic contacts within the cytochrome  $c_3$ -[Fe]-hydrogenase complex. Heme 4 and cytochrome  $c_3$  residues are labeled in red, distal [4Fe-4S] cluster and residues of [Fe]-hydrogenase are labeled in green.

We have recently demonstrated by a similar approach [10] that the same heme (namely heme 4) interacts with Hmc to transfer electrons. In that case heme 4 functions as an electron exit gate of the tetrahemic cytochrome. These results exclude the presence of a ternary complex and support the model where cytochrome  $c_3$  is an electron shuttle between the periplasmic hydrogenase and the membrane-bound Hmc complex. Moreover, the redox partners form transient complexes that are consistent with a high turnover system found in electron-transfer chains.

When one compares the NMR data of the cytochrome  $c_3$ –hydrogenase and cytochrome  $c_3$ –Hmc complexes, five of the 11 residues of cytochrome  $c_3$  that undergo chemical shift variations upon complexation are common to both complexes (C46, D53, D96, T98 and G99). This implies that the same area of the cytochrome is involved in both interacting sites. The models pinpoint important residues at the cytochrome  $c_3$  interface. Besides the hydrophobic residues I36, Y66 and the cysteines, discussed above, we noticed the involvement of several lysines of the loops surrounding heme 4 (K15, K57, K58, K60, K72, K94, K95 and K101). The presence of these charged residues surrounding the interaction site is in agreement with the well-established idea that the electrostatic interactions are the driving force in the formation of complexes involving cytochrome  $c_3$  [21,22]. It is worth noting that a structural comparison and superposition of several different cytochromes  $c_3$  reported earlier [23] has highlighted the presence of these lysine residues in all  $c_3$ -type cytochromes. The role of lysine residues grouped in four loops around the surface-exposed edge of heme 4 in cytochromes has been correlated to the dipole moment, and their different spatial arrangement has been proposed to reflect the difference in specificities towards their physiological partners. However, no specific differences are observed between the involvement of any particular lysines in the complexes of cytochrome  $c_3$  with the [Fe]-hydrogenase or Hmc. In both cases, the above-mentioned lysines are located at the border of the interface, surrounding a hydrophobic patch, and several of them are involved in hydrogen bonds or salt bridges across the surface. This pseudo-specificity has already been described for other electron-transport proteins, such as pseudo-azurin with cytochrome  $cd_1$  nitrite reductase [24]. This finding leads us to conclude that the driving force for cytochrome  $c_3$  to interact with either Hmc or [Fe]-hydrogenase depends more on the respective oxidation states of the involved redox proteins rather than on the interaction of specific residues.

## References

- [1] Widdel, F. and Hansen, T.A. (1991) *The Prokaryotes*, 2nd edn. Springer, New York.
- [2] Traore, A., Fardeau, M.-L., Hatchikian, E.C., LeGall, J. and Bélaich, J.-P. (1983) *Appl. Environ. Microbiol.* 46, 1152–1156.
- [3] Louro, R.O., Catarino, T., LeGall, J. and Xavier, A.V. (1997) *J. Biol. Inorg. Chem.* 2, 488–491.
- [4] Nicolet, Y., Piras, C., Legrand, P., Hatchikian, C.E. and Fonticella-Camps, J.C. (1999) *Structure* 7, 13–23.
- [5] Hatchikian, E.C., Magro, V., Forget, N. and Nicolet, Y. (1999) *J. Bacteriol.* 181, 2947–2952.
- [6] Czjzek, M., Payan, F., Guerlesquin, F., Bruschi, M. and Haser, R. (1994) *J. Mol. Biol.* 243, 653–667.
- [7] Pollock, W.B.R., Loutfi, M., Bruschi, M., Rapp-Giles, B.J., Wall, J.D. and Voordouw, G. (1991) *J. Bacteriol.* 173, 220–228.
- [8] Aubert, C., Brugna, M., Dolla, A., Bruschi, M. and Giudici-Orticoni, M.-T. (2000) *Biochim. Biophys. Acta* 1476, 85–92.
- [9] Pereira, I.A.C., Romão, C.V., Xavier, A.V., LeGall, J. and Teixeira, M. (1998) *J. Biol. Inorg. Chem.* 3, 494–498.
- [10] Czjzek, M., ElAntak, L., Zamboni, V., Morelli, X., Dolla, A., Guerlesquin, F. and Bruschi, M. (2002) *Structure* 10, 1677–1686.
- [11] Palma, P.N., Krippahl, L., Wampler, J.E. and Moura, J.J.G. (2000) *Proteins* 39, 372–384.
- [12] ElAntak, L., Bornet, O., Morelli, X., Dolla, A. and Guerlesquin, F. (2002) *J. Biomol. NMR* 23, 69–70.
- [13] Hatchikian, E.C., Forget, N., Fernandez, V.M., Williams, R. and Cammack, R.C. (1992) *Eur. J. Biochem.* 209, 357–365.
- [14] Wishart, D., Bigam, C., Yao, J., Abildgaard, F., Dyson, J., Oldfield, E., Markley, J. and Sykes, B. (1995) *J. Biomol. NMR* 6, 135–140.
- [15] Ryckaert, J.-P., Ciccotti, G. and Berendsen, H.J.C. (1997) *J. Comput. Phys.* 23, 327–341.
- [16] Zuiderweg, E. (2002) *Biochemistry* 41, 1–7.
- [17] Morelli, X., Dolla, A., Czjzek, M., Palma, P.N., Blasco, F., Krippahl, L., Moura, J.J.G. and Guerlesquin, F. (2000) *Biochemistry* 39, 2530–2537.
- [18] Morelli, X., Palma, N., Guerlesquin, F. and Rigby, A. (2001) *Protein Sci.* 10, 2131–2137.
- [19] Garrett, D.S., Seok, Y.J., Peterkofsky, A., Clore, G.M. and Gronenborn, A.M. (1997) *Biochemistry* 36, 4393–4398.
- [20] Morelli, X., Czjzek, M., Hatchikian, E.C., Bornet, O., Fonticella-Camps, J.C., Palma, N.P., Moura, J.J.G. and Guerlesquin, F. (2000) *J. Biol. Chem.* 275, 23204–23210.
- [21] Stewart, D.E., LeGall, J., Moura, I., Peck, H.D., Xavier, A.V., Weiner, P.K. and Wampler, J.E. (1989) *Eur. J. Biochem.* 185, 695–700.
- [22] Cambillau, C., Frey, M., Guerlesquin, F. and Bruschi, M. (1988) *Proteins* 4, 63–70.
- [23] Czjzek, M., Guerlesquin, F., Bruschi, M. and Haser, R. (1996) *Structure* 4, 395–404.
- [24] Williams, P.A., Fulop, V., Leung, Y.C., Chan, C., Moir, J.W., Howlett, G., Ferguson, S.J., Radford, S.E. and Hajdu, J. (1995) *Nat. Struct. Biol.* 2, 975–982.